

# Power Losses Calculations in Windings of Gapped Magnetic Components: The Extended 2-D Method

Fermín A. Holguín, Roberto Prieto, Rafael Asensi, José A. Cobos

**Abstract**— An improved 2-D equivalent (i2D) analytical calculation method to estimate conductive losses in gapped magnetic components in a wide range of frequencies is presented. In the previous work, which is based on the superposition of losses mechanisms (skin, gap and proximity) in the winding of the component, several expressions to separately evaluate all components of losses were used and the total winding loss could be obtained by the addition of the calculated values. Although the obtained results were in good agreement with finite element analysis (FEA) and measurements this method is limited to conductors with smaller radius than the skin depth at the considered frequency. In this paper the dependence of the wire diameter is eliminated by means of the inclusion of the proximity magnetic field in the calculations while the number of required equations is reduced.

The method is used to evaluate conduction losses in inductors for switched mode power supplies (SMPS) and the results are compared with FEA simulations.

**Index Terms**— Windings losses, windings resistance, magnetic components, air gap.

## I. INTRODUCTION

Winding loss calculation is a very important task in the design process of magnetic components. In components with air gaps, the losses in the windings cannot be accurately calculated with the commonly used methods [1-6], as gap effect over winding losses is not taken into account, so numerical analysis tools, such as FEA tools, are often required for the component characterization [7-9] with the disadvantage of larger design time and the difficulty to implement iterative optimization processes.

The solution presented in [10] accounts for planar conductors in gapped magnetic components and provides analytical expressions to determine the magnetic field at a given position from the gap and, on the other hand, [11], which is for round conductors, uses the mirror-image method [12] to calculate the magnetic field over a conductor that, depending on the desired accuracy, might require a large number of calculations. In [13] a simple solution based on the well-known Dowell's method [1] is proposed, but it can be properly applied only in components whose windings are arranged in a "layered" structure.

In [14] an analytical 2D equivalent method based on the superposition of losses mechanisms (skin, gap and proximity) in the winding of the component was proposed. Although the obtained results are in good agreement with FEA results and measurements, this method is limited to conductors with smaller radius than the skin depth at the considered frequency, for this reason, for a given conductor, the error in the calculations increases as the frequency rises. In this paper, the dependence of the wire diameter is eliminated by means of the inclusion of the proximity magnetic field in the calculations. FEA simulations are used to verify the accuracy of the improved model.

## II. THE 2-D ANALYTICAL MODEL

In [14] the power loss per unit length of a cylindrical conductor under a transverse magnetic field is calculated by means of expression (1) [15], where  $ber$ ,  $bei$ ,  $ber'$  and  $bei'$  are, respectively, the real and imaginary part of the Bessel functions of first kind and their derivatives,  $\sigma$  and  $\mu$  the conductivity and permeability of the conductive material,  $r_0$  is the radius of the conductor and  $H_0$  is the magnitude of the transverse field to the conductor.

$$P = \frac{\pi\mu^2}{\sigma} kr_0 H_0^2 \frac{ber(kr_0)bei'(kr_0) - ber'(kr_0)bei(kr_0)}{\mu^2 [ber(kr_0)]^2 + \mu^2 [bei(kr_0)]^2} \quad (1)$$

Where  $k = \sqrt{w\sigma\mu}$  and  $w$  is the angular frequency. Since the fringing field due to the air gap in a magnetic component (see Figure 1),  $H_g$ , is considered to be two-directional in the plain  $r$ - $z$  in cylindrical coordinates, any conductor affected by this fringing field will be exposed to its two components,  $H_r$  and  $H_z$ , both transverse to the conductor. The field components of  $H_g$  can be calculated, according to [10], with (2) and (3) for  $r$  and  $z$  components respectively, where  $l_g$  is half of the air gap length,  $r$  and  $z$  are the cylindrical coordinates respect of the origin (Figure 1),  $m$  is equal to zero if  $r^2 + z^2 > l_g^2$  and equal to 1 if  $r^2 + z^2 < l_g^2$  and  $H_g \cong 0.9 NI / 2l_g$  with  $N$  and  $I$  equal to the number of turns and peak current through the winding, respectively.

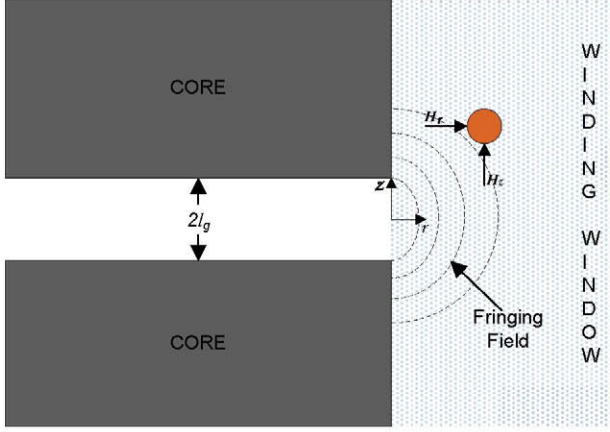


Figure 1. Influence of the fringing field on a conductor in a gapped magnetic component.

$$H_r(r, z) = \frac{H_g}{2\pi} \ln \left[ \frac{r^2 + (z - l_g)^2}{r^2 + (z + l_g)^2} \right] \quad (2)$$

$$H_z(r, z) = -\frac{H_g}{\pi} \left[ \tan^{-1} \left( \frac{2rl_g}{r^2 + z^2 - l_g^2} \right) + m\pi \right] \quad (3)$$

As both components of the fringing field are orthogonal, the dissipated power per unit length in a single conductor due to the influence of the air gap can be expressed as the vectorial sum of the loss due to both components,  $P_r$  and  $P_z$  (equation 4), that are calculated by means of (1) using (2) or (3) as  $H_\theta$  respectively.

$$P_g(W/m) = \sqrt{P_r^2 + P_z^2} \quad (4)$$

The effect of near conductors in the proximity and the effect of the current flowing through the conductor itself (proximity and skin effects respectively), in [14] are evaluated by means of expression (5), from [15], where  $\delta$  is the skin depth,  $J_0$  is the DC current density and  $x$  is the distance between conductors. Then, the total dissipated power per unit length of a cylindrical conductor in a gapped magnetic component can be expressed as the sum of (4) and (5) and the equivalent resistance is obtained dividing by the squared of the RMS current through the winding.

$$P_{prox}(W/m) = \frac{J_0^2 \pi r^2}{\sigma} \left[ 1 + \frac{1}{48} \left( \frac{r}{\delta} \right)^4 \left[ 1 + 12 \left\{ \left( \frac{r}{x} \right)^2 + \frac{1}{6} \sum_{n=2}^{\infty} \frac{1}{(2n-3)} \left( \frac{r}{x} \right)^{2n} \right\} \right] \right] \quad (5)$$

Since (5) is a simplified expression, the radius of the conductor is considered to be relatively small compared with the skin depth at the given frequency. This is applicable only in windings that meet this condition, and it becomes evident that the error will increase as frequency rises and the radius of the conductor is no longer smaller than the skin depth, as it is

the case of the calculation of winding losses in power electronics application where the harmonic content of the current through the component can be very important.

### III. THE IMPROVED 2-D ANALYTICAL METHOD

Proximity and gap effects, which in the described 2D method are evaluated separately, are actually the same effect (external fields) and can be calculated using the same expression. This way, we need to calculate skin and proximity components in order to estimate the total winding loss. The equivalent resistance per unit length due to the skin effect can be calculated by means of expression (6), from [15], and the proximity component, which includes the fringing and proximity fields, can be evaluated using (1) just including the proximity and fringing field information as  $H_\theta$ .

$$R_s(\Omega/m) = Re \left[ \frac{j^2 k}{2\pi r_0 \sigma} \frac{BesselJ_0(j^2 k r_0)}{BesselJ_1(j^2 k r_0)} \right] \quad (6)$$

If we assume a magneto-static field condition and consider the fringing and proximity fields independent of each other (in order that superposition theorem could be used), the Biot-Savart law (expression 7) can be used to calculate the magnetic field that is affecting a single conductor of length  $L$  due to the electric current  $I$  flowing through a near conductor at a position  $x$  by means of expression (8) (Figure 2), where  $\hat{x}$  is an unitary vector in the direction of  $x$ .

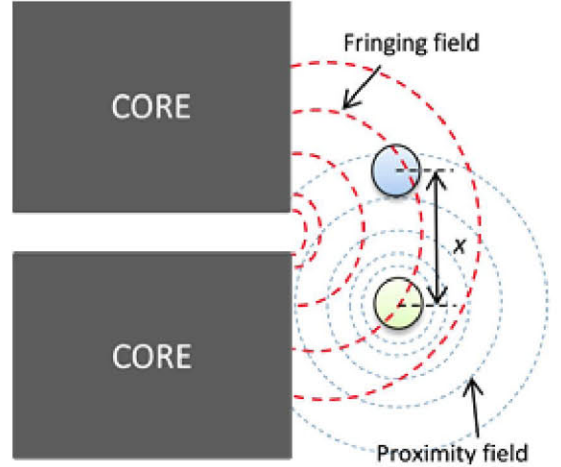


Figure 2. Representation of both, fringing and proximity, fields in a gapped magnetic component.

$$d\vec{H} = \frac{1}{4\pi} \frac{I d\vec{l} \times \hat{x}}{x^2} \quad (7)$$

$$\vec{H} = -\frac{I}{2\pi x} \frac{L}{\sqrt{L^2 + x^2}} (\hat{x}) \quad (8)$$

At this point, just as the 2D method,  $P_r$  and  $P_z$  can be calculated assuming the external field,  $H_0$ , as the sum of the corresponding components of the fringing and proximity fields. This way the external field becomes (9) and the total loss per unit length of the considered conductor can be obtained as the sum of (10), whose components are evaluated by means of (1) with corrected values of the magnetic field ( $H'_0$ ), and (6) multiplied by the square of the RMS current through the winding.

$$H_g + H_p = (H_{gr} + H_{pr}) + (H_{gz} + H_{pz}) = H'_0 \quad (9)$$

$$P = \sqrt{P_r'^2 + P_z'^2} \quad (10)$$

#### IV. RESULTS

The results of the proposed i2D model are compared with FEA. As a practical case, consider the inductors shown in Figure 4 as four possible designs of an inductor for a hypothetic SMPS in discontinuous conduction mode working at 400 kHz (see the waveform of the current in Figure 4e).

The inductors were designed and modeled with the aid of the magnetic component design and FEA tools ANSYS PExprt and ANSYS MAXWELL respectively for the hypothetic operating conditions specified in table 2. The magnetic materials of the core in the inductors 3a/3b/3d and 3c are, respectively, 3C95 and 3F3 from Ferroxcube with a relative permeability of 3000 and 2000. A copper conductivity of 45.25E6 S/m was used in all the calculations and FEA simulations.

For simplicity, 2D axis-symmetric analysis is used for the FEA simulations. The components were modeled in the FEA tool using the structure transformation described in [16]. The 2D axis-symmetric FEA model of the inductor 3a is shown in Figure 3, where the blue area is the solution space in which the vector potential,  $A$ , has been set to zero in its outer edges. After modeled, the inductors were simulated at different frequencies that correspond to the first 30 harmonics of the current in the Figure 4e (the harmonic content of the current waveform is given in the table 2). The same modelling strategy has been applied to the others inductors of the Figure 4.

Table 1. Design conditions of the considered inductors.

Positive Voltage	48 V
Negative voltage	120 V
Average current	4 A
Current ripple	14 A
Inductance	3.5 $\mu$ H
Frequency	400 kHz
Duty cycle	0.41

The analytical results for components 3a, 3b, 3c and 3d (including the skin depth approach which does not include the effect of the fringing field nor the proximity effect) are

compared with FEA in table 3. The analytical (both 2D and i2D) and FEA calculated equivalent resistance of the inductor 3b are compared in Figure 5, where the error that is introduced as the frequency increases in the 2D method is illustrated. It can be seen that the improved 2D analytical model that were used for computing the equivalent resistance of the windings shows much better results than the previous 2D method with respect to FEA results, which was accurate for the fundamental harmonic, but inaccurate for high order harmonics.

Table 2. Harmonic content of the excitation current.

Order of the harmonic	Peak current (A)	Order of the harmonic	Peak current (A)
1	5.966	16	0.044
2	2.293	17	0.018
3	1.138	18	0.013
4	0.624	19	0.014
5	0.206	20	0.016
6	0.100	21	0.027
7	0.108	22	0.017
8	0.127	23	0.017
9	0.141	24	0.003
10	0.085	25	0.003
11	0.065	26	0.013
12	0.003	27	0.011
13	0.023	28	0.015
14	0.048	29	0.007
15	0.040	30	0.006

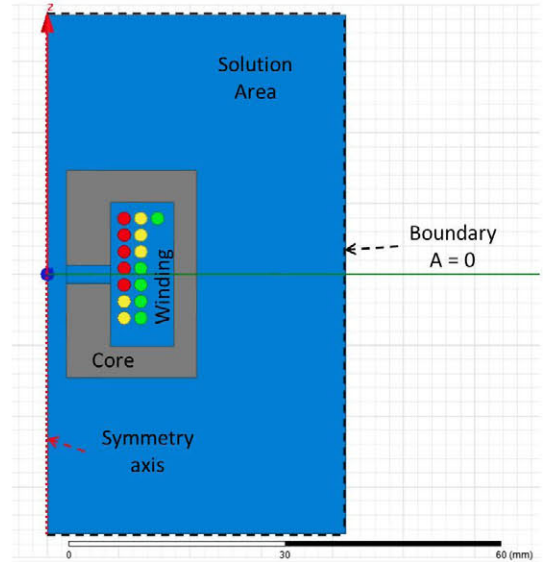
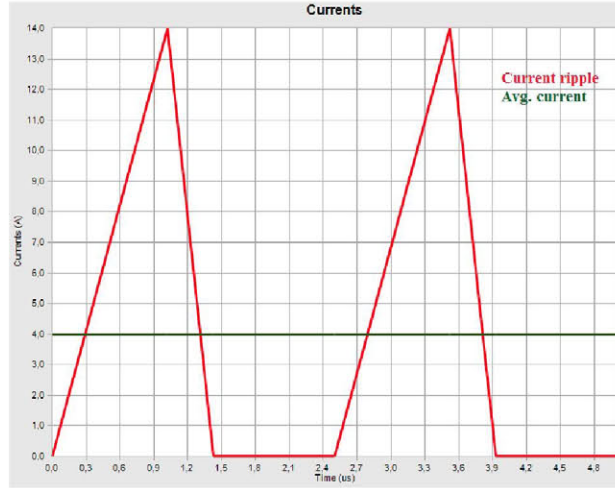
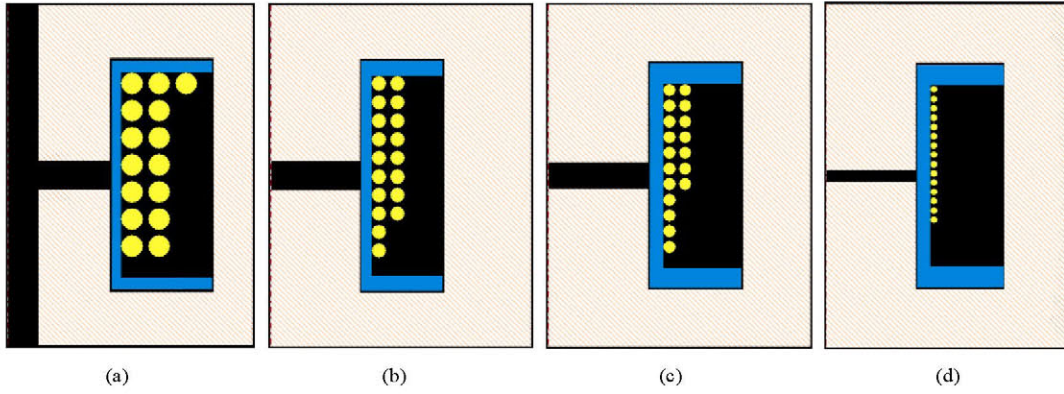


Figure 3. Representation of the 2D axis-symmetric FEA model of the inductors.



(e)  
Figure 4. Axisymmetric representation of inductors with (a) 2.55mm air gap, 5 AWG13 turns (3 parallel) in a P42/29 core, (b) 2.13 mm air gap, 6 AWG18 turns (3 parallel) in a RM12/I core, (c) 1.47 mm air gap, 6 AWG22 turns (3 parallel) in a RM10/I core, (d) 578.35  $\mu\text{m}$  air gap, 5 AWG28 turns (3 parallel) in a RM8/I core and (e) hypothetic current waveform of the inductor.

Table 3. Comparison between analytical and FEA calculated power loss.

Inductor	Power Loss (W)				Relative error (%)		
	skin	2D	i2D	FEA	skin	2D	i-2D
<b>3a</b>	119.32E-3	20.61	2.71	2.94	95.94	601.02	7.82
<b>3b</b>	205.39E-3	7.22	4.02	4.05	94.93	78.27	0.74
<b>3c</b>	322.30E-3	4.64	3.74	3.99	91.92	16.29	6.27
<b>3d</b>	592.61E-3	2.23	2.02	2.00	70.37	11.50	1.00

## V. CONCLUSIONS

An improved analytical method to calculate winding loss in gapped magnetic components is proposed. As the calculation of the “proximity” component of the winding loss has been improved, the dependence of the results with the conductor diameter and frequency is eliminated so the accuracy and range of validity of the previous method has been increased.

Although it is a simplified method (since the fringing and proximity fields are considered to be “independent” and are calculated by separate) an error is introduced in the calculation of the fields, thus, in the calculation of losses. Even so, the obtained results, compared with FEA, are very good and the method can be used to estimate losses in inductors for SMPS applications where the harmonic content of the excitation current might be important and, for a given selected wire, the 2D method could be inappropriate.

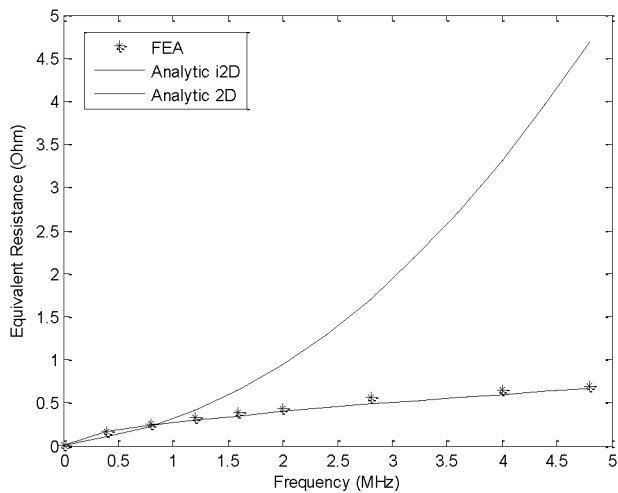


Figure 5. Comparison of the analytical and FEA calculated equivalent resistance vs. frequency of the inductor 3b.

#### REFERENCES

- [1] P.L. Dowell, "Effects of eddy currents in transformer windings", *Proceedings of the IEE*, vol. 113, no. 8, pp. 1387–1394, Aug. 1966.
- [2] Xi Nan and Charles R. Sullivan, "An improved calculation of proximity effect loss in high frequency windings of round conductors", *34th Annual IEEE Power Electronics Specialists Conference*, 2003, vol. 2, pp. 853–860.
- [3] Xi Nan and Charles R. Sullivan, "Simplified high-accuracy calculation of eddy-current loss in round-wire windings", *35th Annual IEEE Power Electronics Specialists Conference*, 2004, vol. 2, pp. 873 – 879.
- [4] F. Robert, P. Mathys and J. P. Schauwers "A closed-form formula for 2-D ohmic losses calculations in SMPS transformer foils", *IEEE Transactions on Power Electronics*, vol. 16, pp. 437-444, May 2001.
- [5] J. A. Ferreira, "Improved analytical modeling of conductive losses in magnetic components", *IEEE Transactions on Power Electronics*, vol. 9, no. 1, pp. 127–31, Jan. 1994.
- [6] Mohammad Etemadrezaei and Srdjan M. Lukic "Equivalent complex permeability and conductivity of litz wire in wireless power transfer systems", *IEEE Energy Conversion Congress and Expositions*, 2012, pp. 3833-3840.
- [7] R. Asensi, J.A. Cobos, O. García, R. Prieto and J. Uceda "A full procedure to model high frequency transformer windings", *25th Annual IEEE Power Electronics Specialists Conference*, 1994, vol. 2, pp. 856-863.
- [8] R. Asensi, R. Prieto, J.A. Cobos and J. Uceda "Modeling high-frequency multiwinding magnetic components using finite-element analysis", *IEEE Transactions on Magnetics*, vol. 43, no. 10, pp. 3840-3850, 2007.
- [9] R. Prieto, R. Asensi, C. Fernandez, J.J.A. Oliver and J.A. Cobos, "Bridging the gap between FEA field solution and the magnetic component model", *IEEE Transactions on Power Electronics*, vol. 22, no. 3, pp. 943-951, 2007.
- [10] Waseem A. Roshen "Fringing Field Formulas and Winding Loss Due to an Air Gap", *IEEE Transactions on Magnetics*, vol. 43, no. 8, pp. 3387-3394, August 2007.
- [11] Chen Wei, Huang Xiaosheng and Zheng Juanjuan "Improved winding loss theoretical calculation of magnetic component with air gap", *7th International Power Electronics and Motion Control Conference*, 2012, vol. 1, pp. 471-475.
- [12] Jiankun Hu and Charles R. Sullivan "Optimization of shapes for round-wire high-frequency gapped-inductor windings", *33th Annual IEEE Industry Applications Conference*, 1998, vol. 2, pp. 907-912.
- [13] Fermin A. Holguin, R. Asensi, R. Prieto and J.A. Cobos, "Simple analytical approach for the calculation of winding resistance in gapped magnetic components", *29th Annual IEEE Applied Power Electronics Conference and Exposition*, 2014, pp. 2609-2614.
- [14] Fermin A. Holguin, R. Prieto, R. Asensi and J.A. Cobos, "Power losses calculations in windings of gapped magnetic components", *29th Annual IEEE Applied Power Electronics Conference and Exposition*, 2014, pp. 2605-2608.
- [15] J. Lammeraner and M. Stalf "Eddy Currents", ILIFFE books LTD., 1966, chapter 6 and 7.
- [16] R. Prieto, J. A. Oliver and J. A. Cobos, "Study of non-axisymmetric magnetic components by means of 2D FEA solvers," in *IEEE 36th Power Electronics Specialists Conference*, 2005, pp. 1074-1079.